4.
BROADBAND DUAL ANTENNA STRUCTURE FOR UHF RFID TAGS

4.1. Introduction

Globally the frequency band for UHF RFID system is ranged from 840 to 960 MHz, but each country has its own frequency allocation. For example, the RFID UHF bands are 840–845 MHz and 920– 925 MHz in China, 866–869 MHz in Europe, 902–928 MHz in North and South America, and 950–956 MHz in Japan. Therefore, it is desirable to design dual antenna structure with a broadband capability to cover multiple RFID UHF bands. Recently, various broadband tag antennas have been reported [Chen and Tsao (2010), Santiago *et al*. (2013), Mo *et al*. (2008), Lai and Li (2011)]. In [Chen and Tsao (2010] tag antenna covered 889-932 MHz band while in [Santiago *et al.* (2013), Mo *et al.* (2008), Lai and Li (2011)], the half power bandwidth is from 840-960, 842-975, and 840-960 respectively, and all of them utilized single antenna for both receiving and backscattering modes.

In this chapter, a single sided broadband antenna for RFID tag is presented which covers 913-960 MHz in UHF bands. The proposed tag antenna consists of two independent antennas one for receiving (Antenna-I) and the other for backscattering (Antenna-II) which enhances the read range [Chen *et al.* (2011)b]. The configuration of receiving and backscattering antenna is given in the next section. The performance of proposed antenna is evaluated in terms of RCS, gain, and read range. The antenna design concepts along with simulated and measured results are discussed in the following sections.

4.2. Antenna Configuration

The antenna configuration and fabricated a prototype of the proposed broadband dual antenna for RFID tag is shown in Figures 4.1(a) and 4.1(b), respectively in which one antenna for receiving (Antenna-I) and the other for backscattering (Antenna-II). The Antenna-I is made up of two rectangular patches

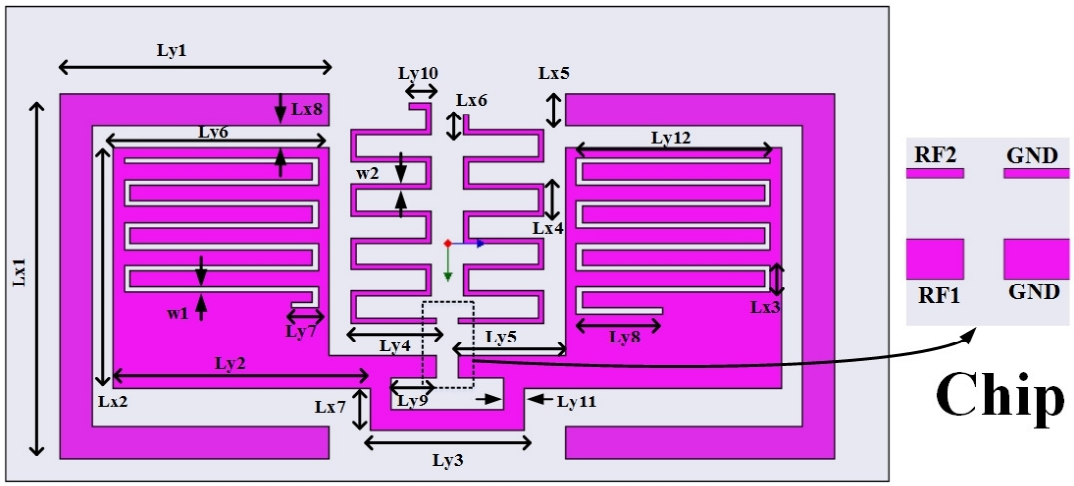

(a)

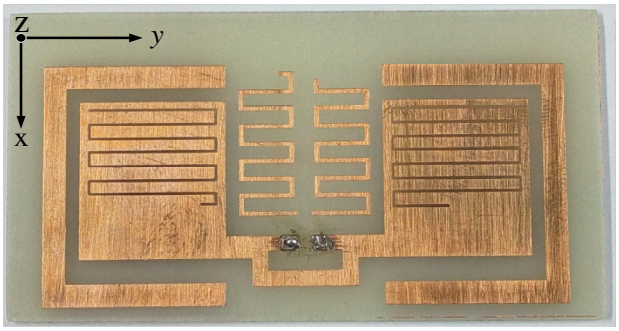

(b)

Figure 4.1: (a) Geometry of proposed dual antenna with zoomed section of the feed connections and (b) fabricated prototype of proposed dual tag antenna.

loaded with two asymmetric meandered line slots connected with T-matching structure. The whole structure is electromagnetically coupled with two C-shaped patches which help in the further tuning of the input impedance of Antenna-I. In a coarse design, the Antenna-I is a half wavelength structure for UHF 925 MHz frequency (Figure 4.1). The Antenna-II is made up with two asymmetric meandered lines in the dipole configuration. It is fabricated on a low cost FR4 substrate having dielectric constant (ε_r) 4.4, loss tangent (*tan* δ=0.018), and thickness 1.6 mm. The proposed dual antenna structure works with a tag IC of four terminals. The four terminals of tag IC for dual antenna structure are denoted as RF1, RF2, and two grounds corresponding to Antenna-I and Antenna-II. RF1 and corresponding ground are connected to the signal terminals of the receiving

antenna and RF2 and its ground is connected to the signal terminals of the backscattering antenna. Antenna-II is utilized for backscattering of 925 MHz to achieve maximum impedance difference between open and short circuit during operations of tag, which helps to maximize the read range. The actual overall size of the designed antenna is 44×82 mm^2.

To design a presented RFID tag antenna, initially, coarse dimensions are chosen corresponding to half wavelength structure which contains two rectangular patches loaded with asymmetric meandered slot connected with a T-matching network to achieve adjacent resonances within UHF band. Further, the antenna is electromagnetically coupled to the C-shaped parasitic element for fine tuning of the input impedance of the tag antenna corresponding to 915 MHz and 925 MHz. Figure 4.2 shows the evolution of the antenna with and without C-shaped structures.

4.3. Result and Discussion

The presented antenna is designed for Alien IC Higgs tag chip which has an input impedance of 13.5-j110 Ω at 925 MHz [Higgs 4 product overview, Alien Technology, 2012]. All the simulations are performed using the Ansys high frequency structure simulator (HFSS) [HFSS ver. 14.0]. The optimized values of shape parameters of the presented antenna are shown in Table 4.1.

Table 4.1: Optimized shape parameters of the proposed RFID antenna

Antenna parameter	Value (mm)	Antenna parameter	Value (mm)	Antenna parameter	Value (mm)
Lx1	34	Ly1	25	Ly7	2.5
Lx2	22.4	Ly2	23.8	Ly8	8
Lx3	2.5	Ly3	14.4	Ly9	4.2
Lx4	3	Ly4	8	Ly10	2
Lx5	3	Ly5	10	Ly11	2
Lx6	2	Ly6	20	Ly12	18
Lx7	4				

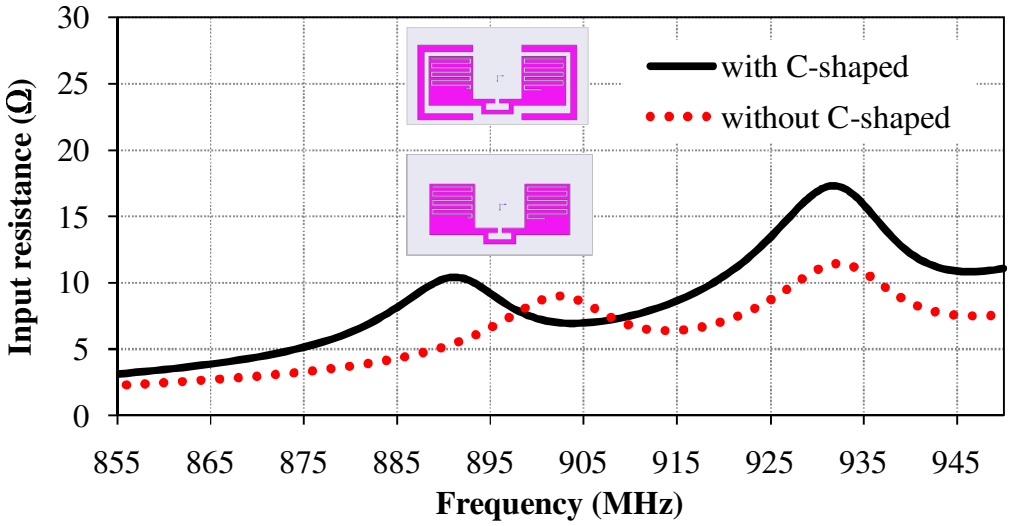

(a)

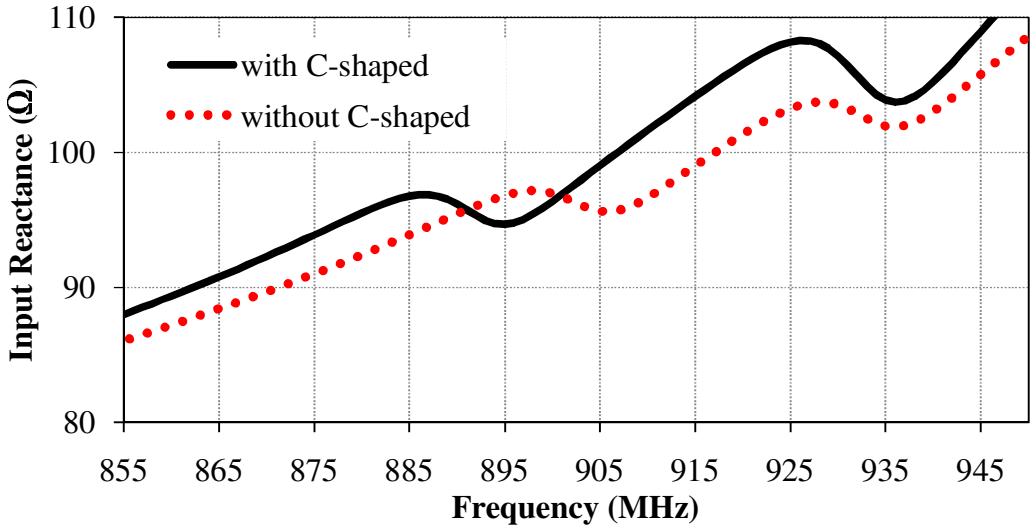

(c)

Figure 4.2: Evolution of the broadband receiving antenna (Antenna-I) (a) input resistance and (b) input reactance

4.3.1 Parametric Study

4.3.1.1. *Receiving antenna*

The main objective of the parametric study of the receiving antenna in the presence of backscattering antenna is to achieve proper complex conjugate of the chip. To achieve complex conjugate of the chip, at a time one of the shape

parameters of the receiving antenna is varied by keeping other shape parameters are fixed at their optimized value as shown in Table 4.1. To achieve these optimized values; initially, the coarse design of the antenna is considered based on the half wavelength concept of the radiating element.

Variations of simulated input impedance and power reflection coefficient (PRC) of receiving Antenna at 925 MHz by varying *Lx*7, *Ly*7 and *Ly8* are presented in Figures 4.3 to 4.6. It is observed that the input impedance of the antenna changes by variation of *Lx*7, *Ly*7 and *Ly8*. To make asymmetric meandered lines, two different values of *Ly*7 and *Ly8* are chosen which is responsible for two adjacent resonances. However, these two resonances are close together, therefore, by changing each length, both resonance frequencies changes. Further, it is also observed from Figure 4.3 that for the optimum values, the real and imaginary part of input impedances are 13.5 Ω and j108 Ω at 925 MHz. It is in close proximity to the complex conjugate of the chip impedance i.e., 13-j110Ω; therefore, maximum power will transfer to antenna which is also corroborated from the PRC variation.

Further, the effect of C-shaped parasitic elements on the impedance of the Antenna-I is investigated by tuning the Ly1, Lx1, Lx8 and Lx5 are shown in Figures 4.7 – 4.10. It is observed that for the variation of Ly1 and Lx1, the input impedance changes in a similar manner with the increase of Ly1 and Lx1. It is interestingly noted that initially the resistance and reactance values at 915 MHz and 925 MHz increases with the increase of the Ly1 and Lx1 at optimized values thereafter it decreases with the increase of the same. In the case of Lx8, the values of the resistance and reactance at 915 MHz and 925 MHz rapidly increases with the increase of Lx8 at optimized value thereafter rapidly decrease with the increase of the Lx8. With the increase of Lx5 both resistance and reactance values at 915 MHz and 925 MHz increases.

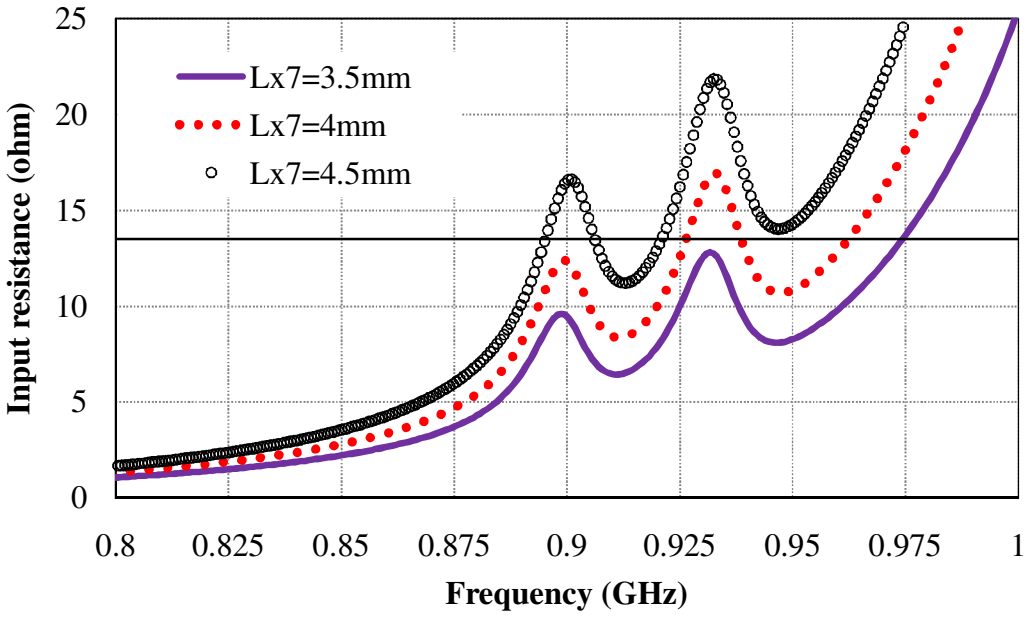

(a)

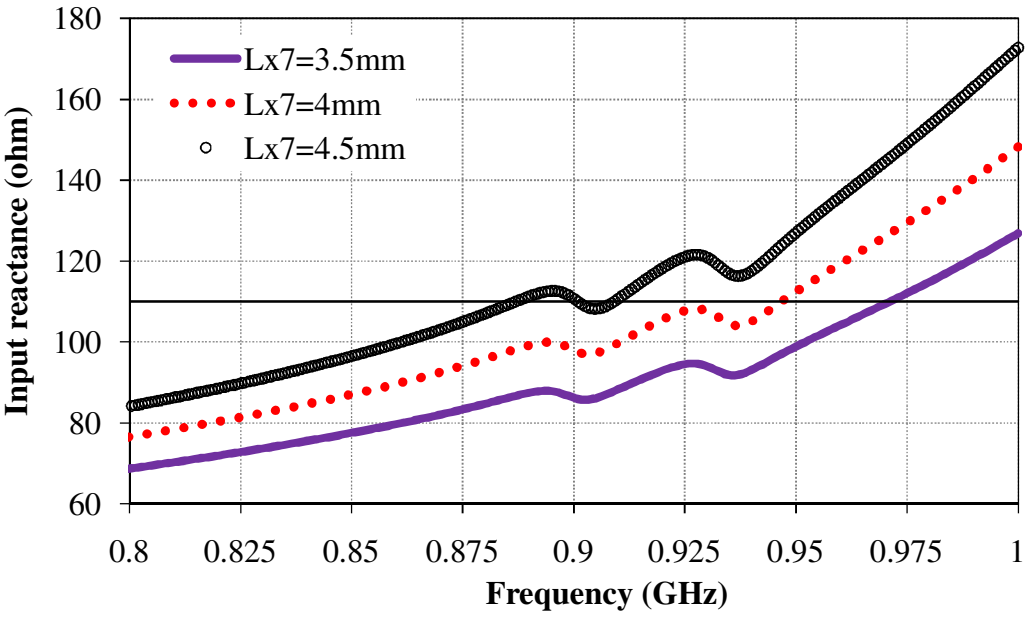

(b)

Figure 4.3: (a) Simulated Input resistance and (b) Input reactance of receiving antenna by tuning *Lx7*

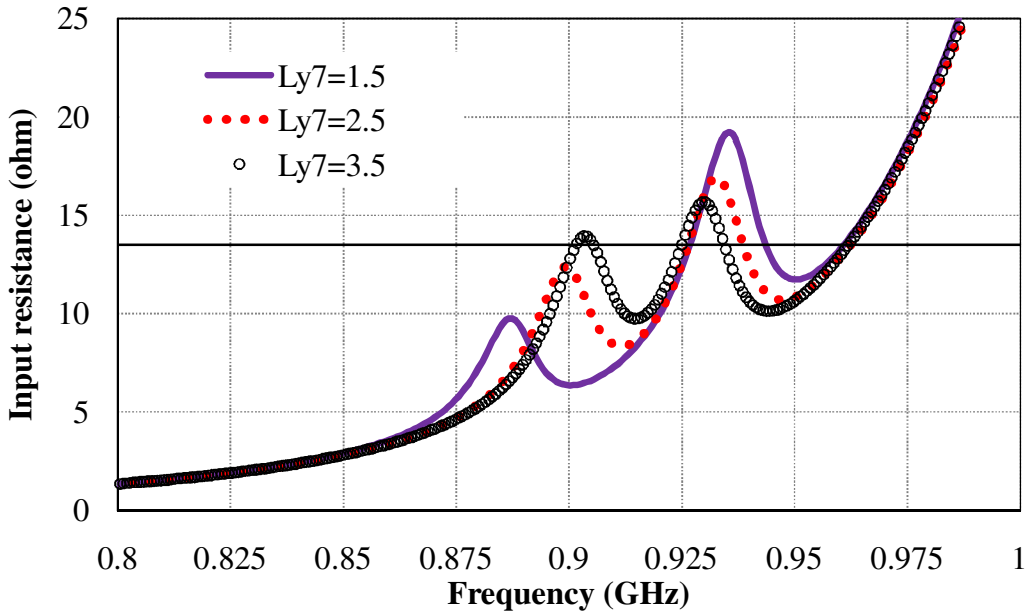

(a)

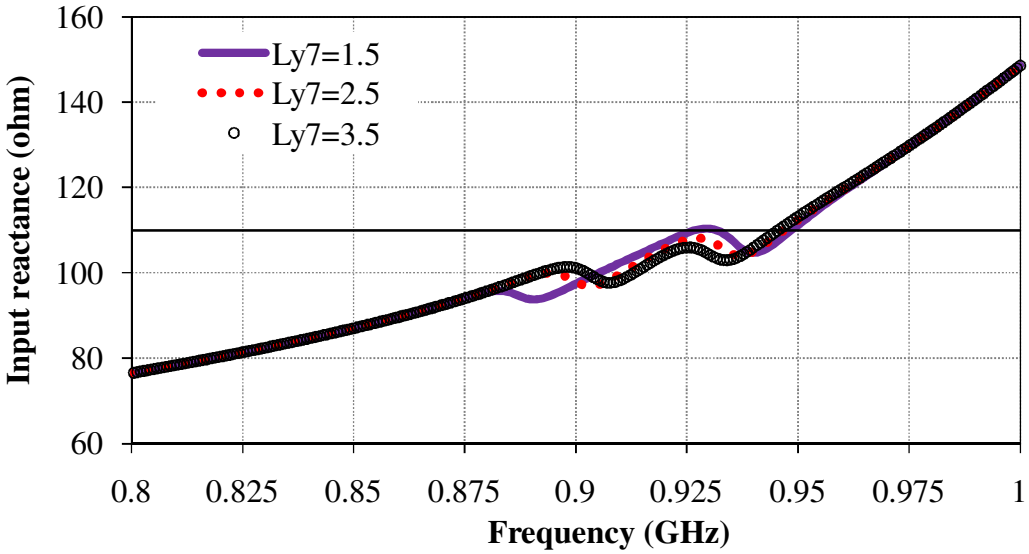

(b)

Figure 4.4: (a) Simulated Input resistance and (b) Input reactance of receiving antenna by tuning Ly7

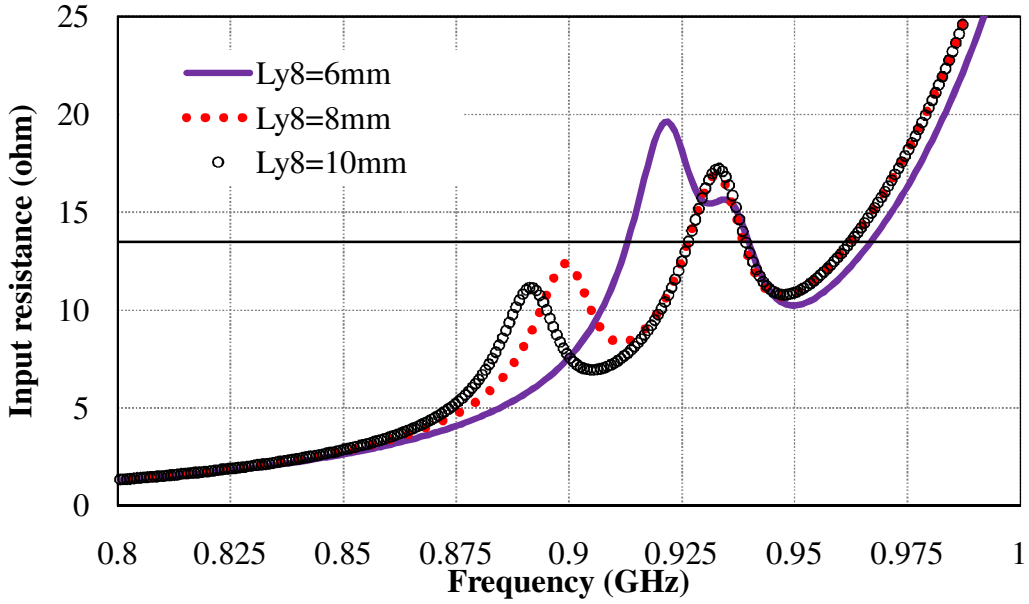

(a)

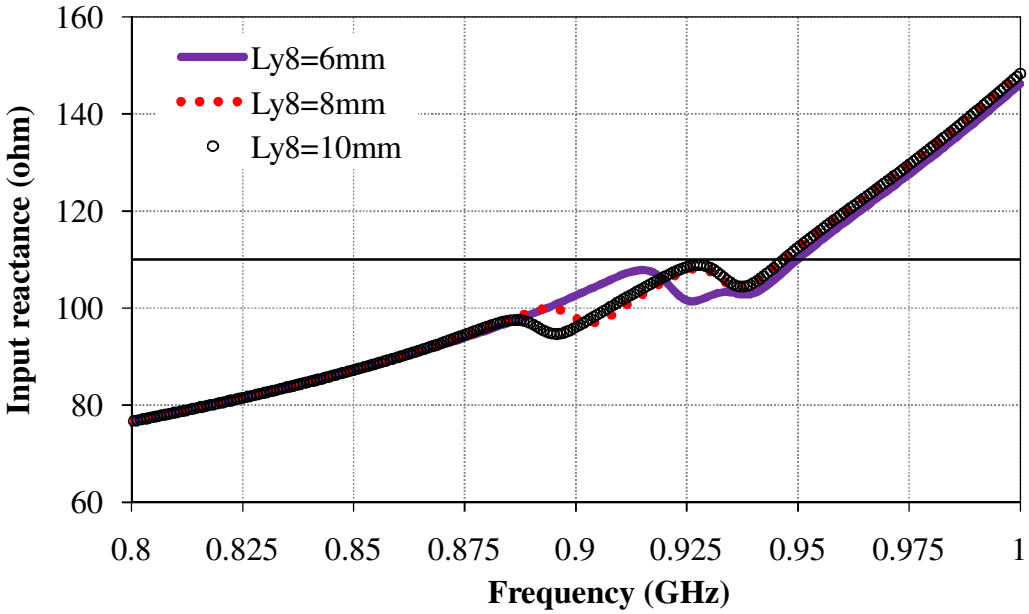

(b)

Figure 4.5: (a) Simulated Input resistance and (b) Input reactance of receiving antenna by tuning Ly8

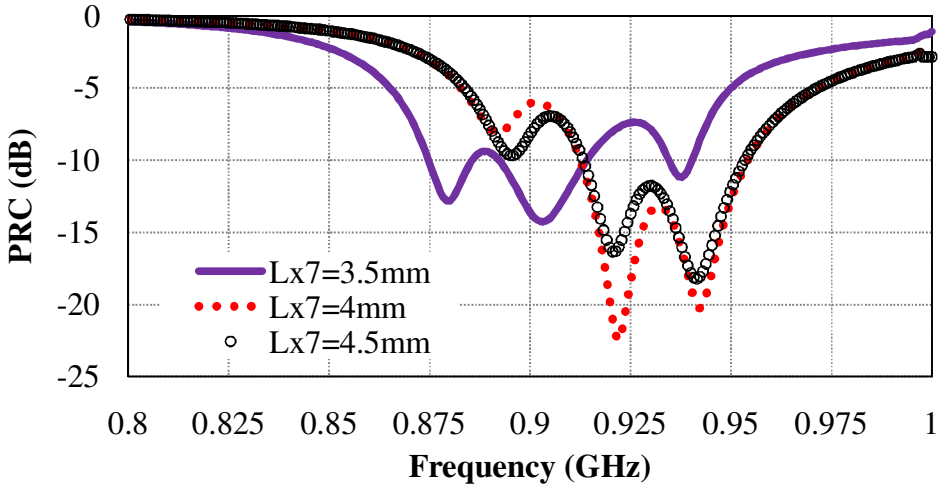

(a)

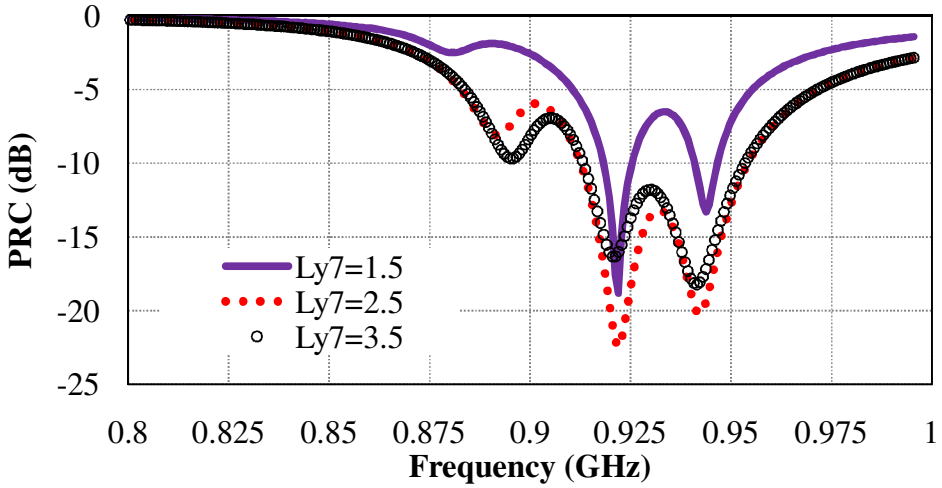

(b)

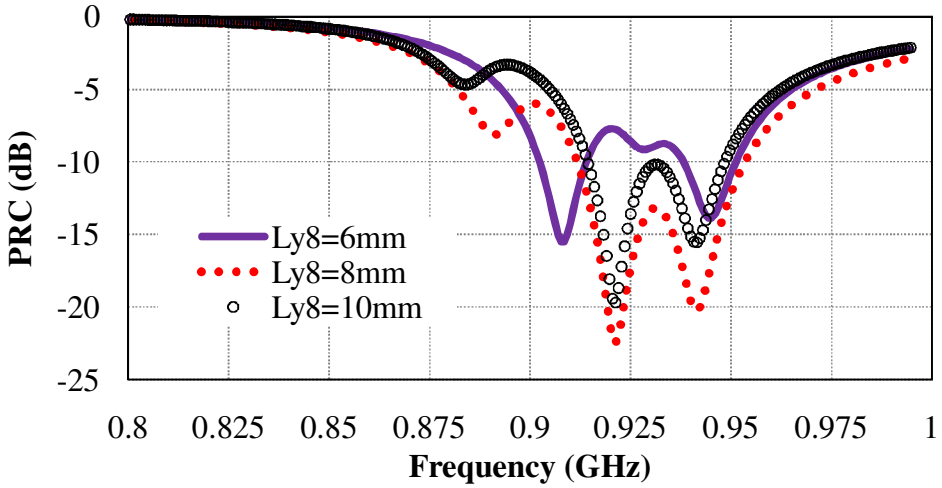

(c)

Figure 4.6: Simulated power reflection coefficient of receiving antenna by tuning: (a) Lx7 (b) Ly7 and (c) Ly8.

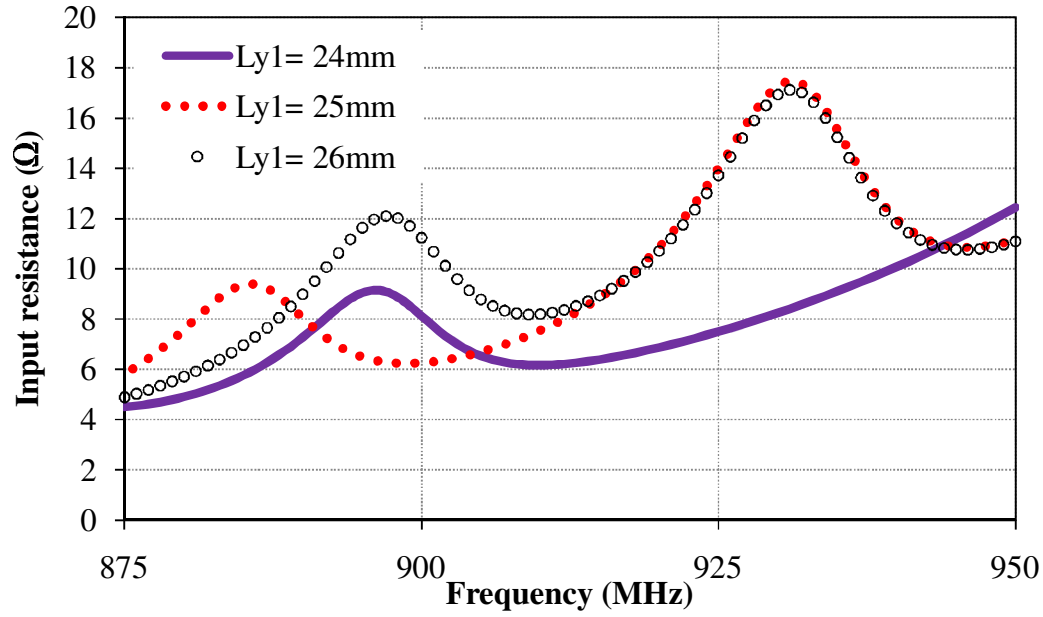

(a)

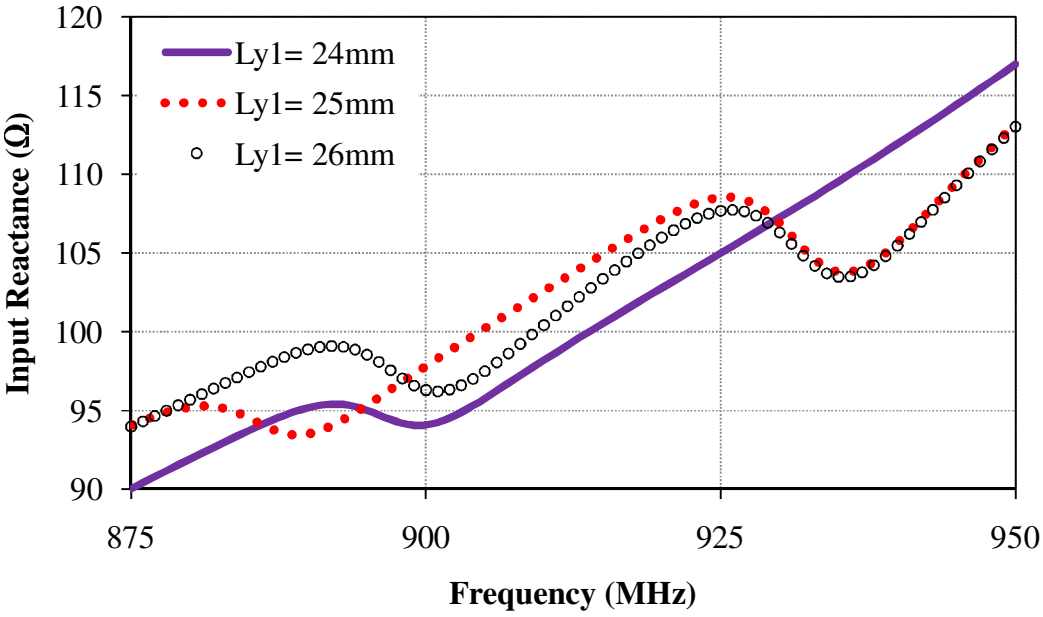

(a)

Figure 4.7: (a) Simulated Input resistance and (b) Input reactance of receiving antenna by tuning Ly1

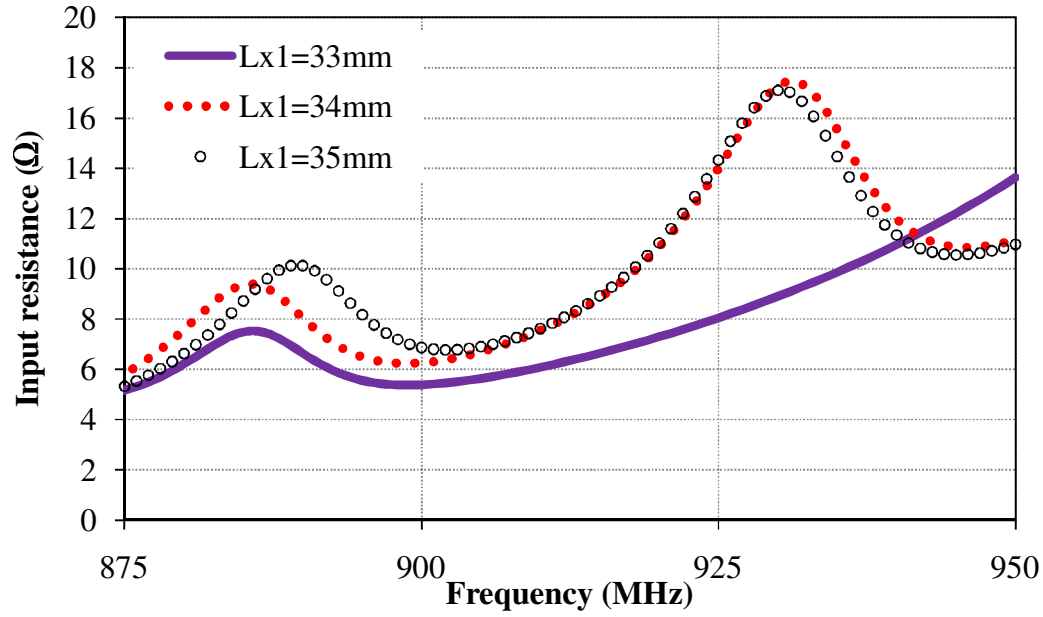

(a)

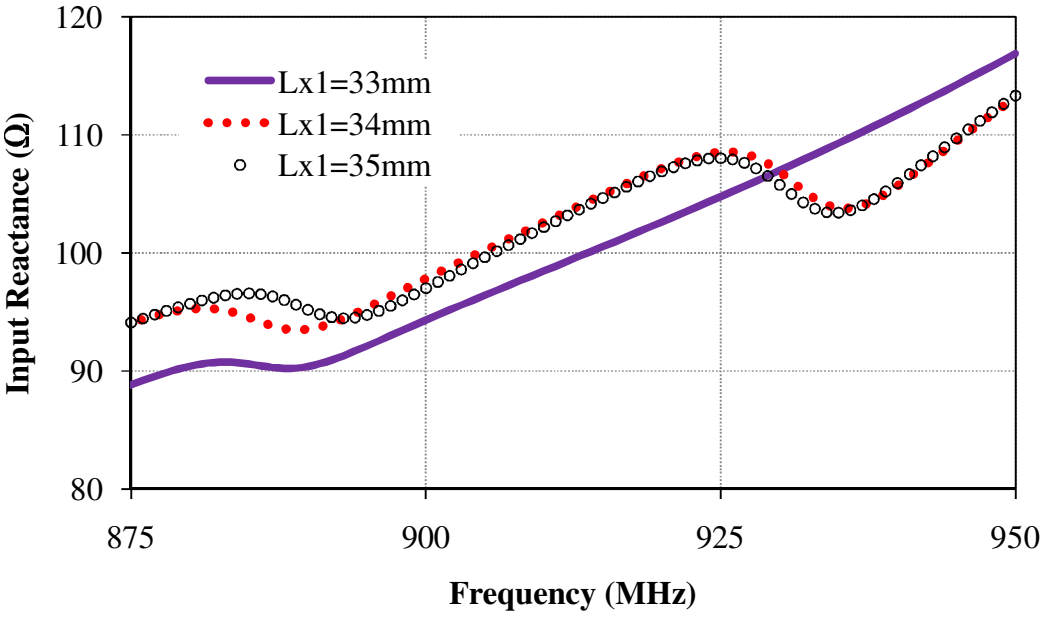

(b)

Figure 4.8: (a) Simulated Input resistance and (b) Input reactance of receiving antenna by tuning Lx1

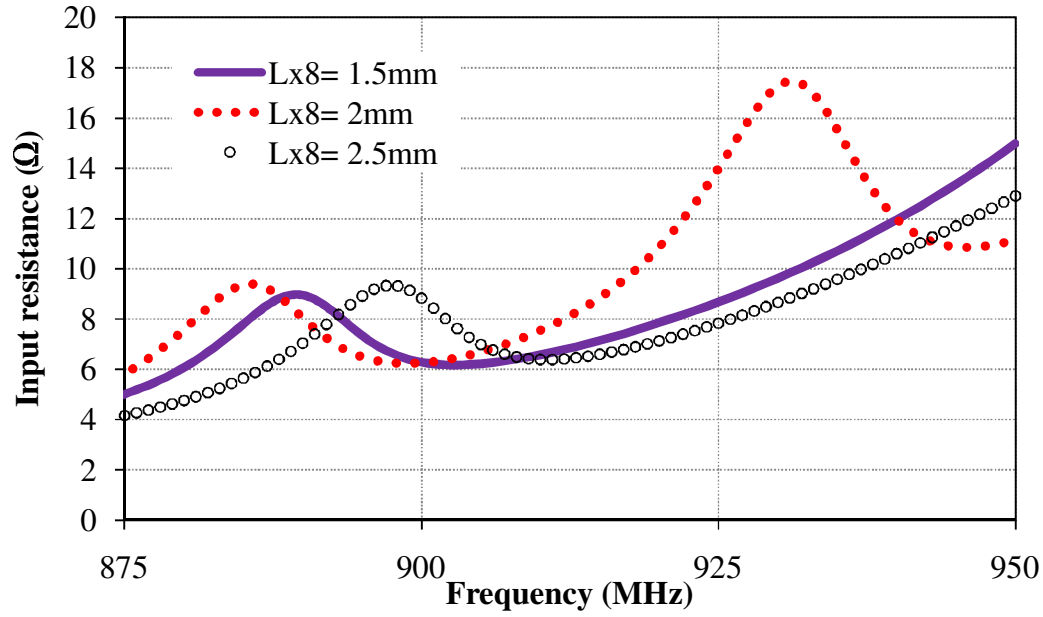

(a)

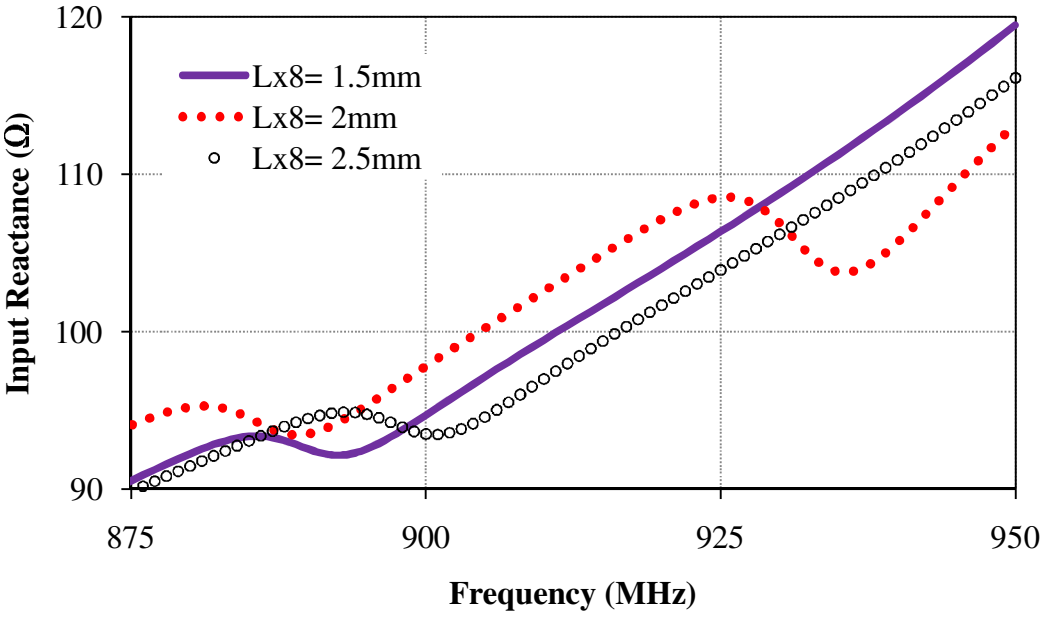

(b)

Figure 4.9: (a) Simulated Input resistance and (b) Input reactance of receiving antenna by tuning Lx8

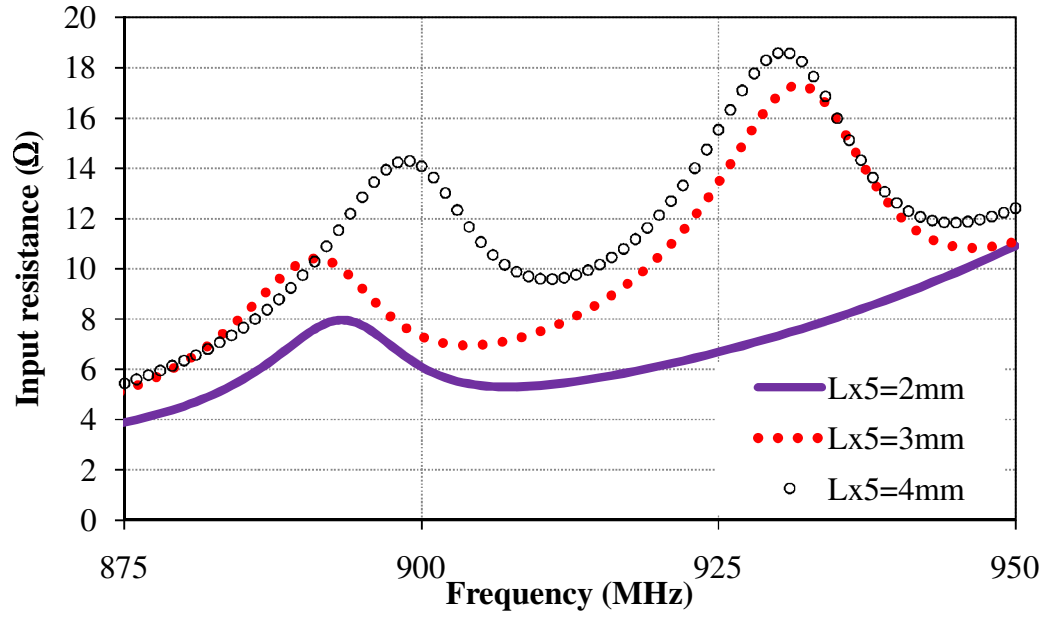

(a)

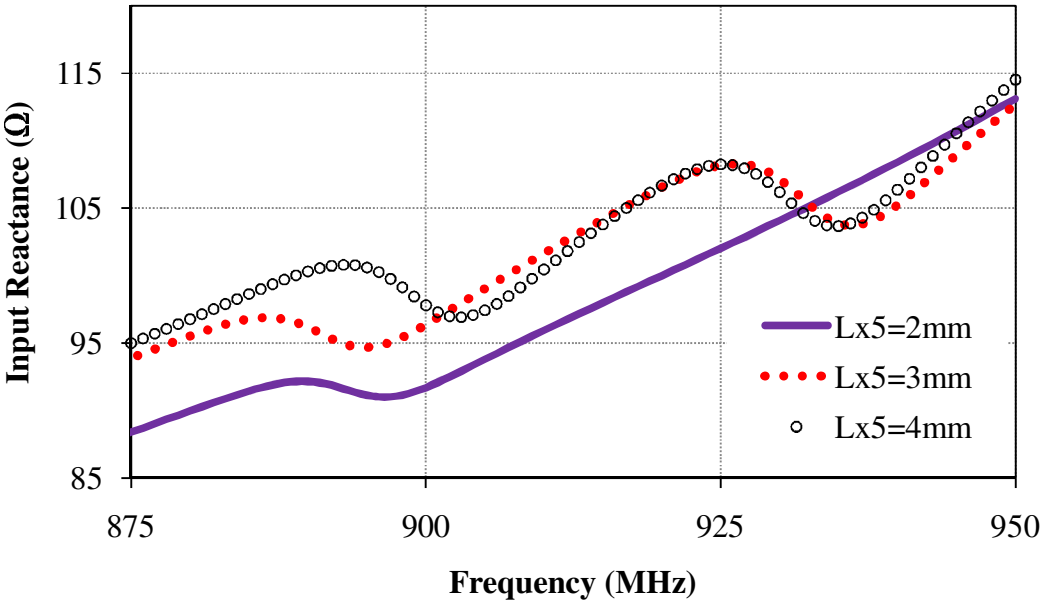

(b)

Figure 4.10: (a) Simulated Input resistance and (b) Input reactance of receiving antenna by tuning Lx5

The thickness (Ly11) and the length (Ly3) of the T-matching network structure also show the significant effect on the input impedance of the receiving antenna which is shown in Figures 4.11 and 4.12 respectively. It is observed from Figure 4.11 that the real and imaginary part of the input impedance of receiving

antenna decreases significantly with the increase of Ly11 in the UHF band. It is observed from Figure 4.13 that the input impedance increases significantly with the increase of Ly3.

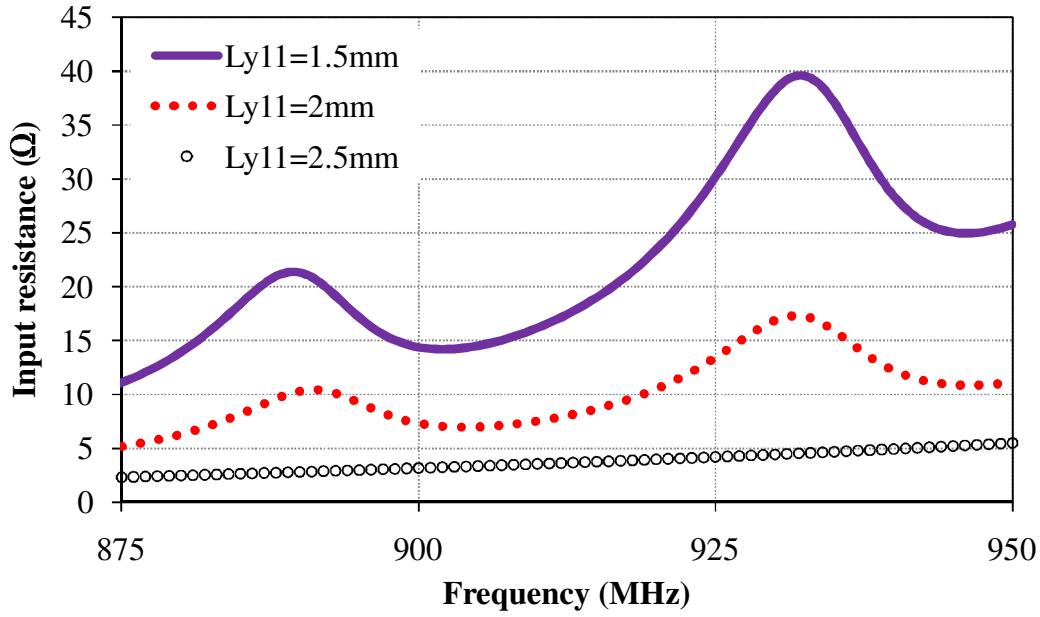

(a)

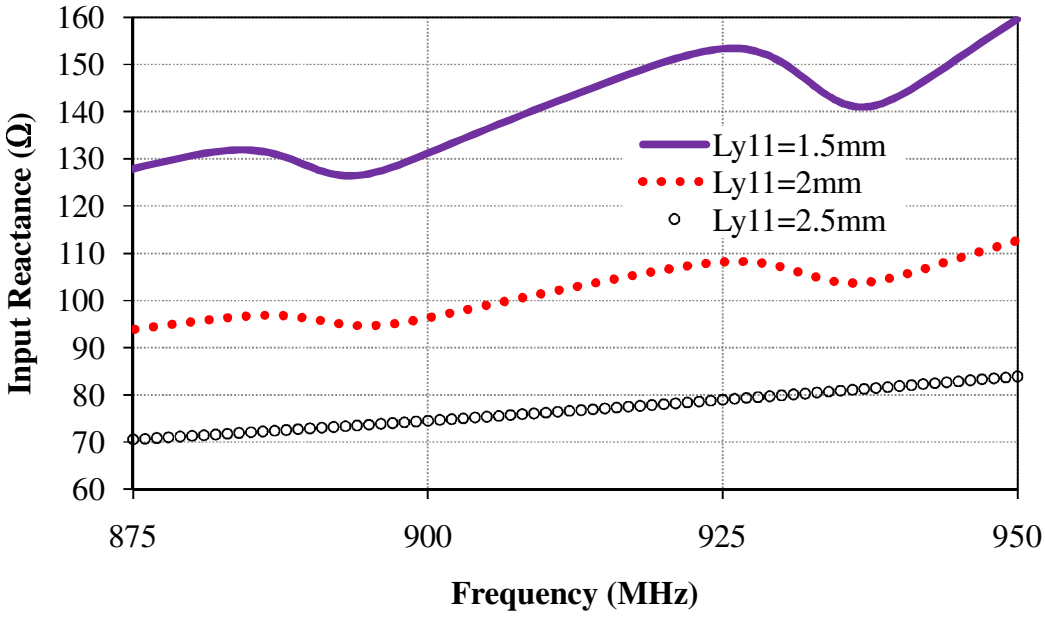

(b)

Figure 4.11: (a) Simulated Input resistance and (b) Input reactance of receiving antenna by tuning Ly11

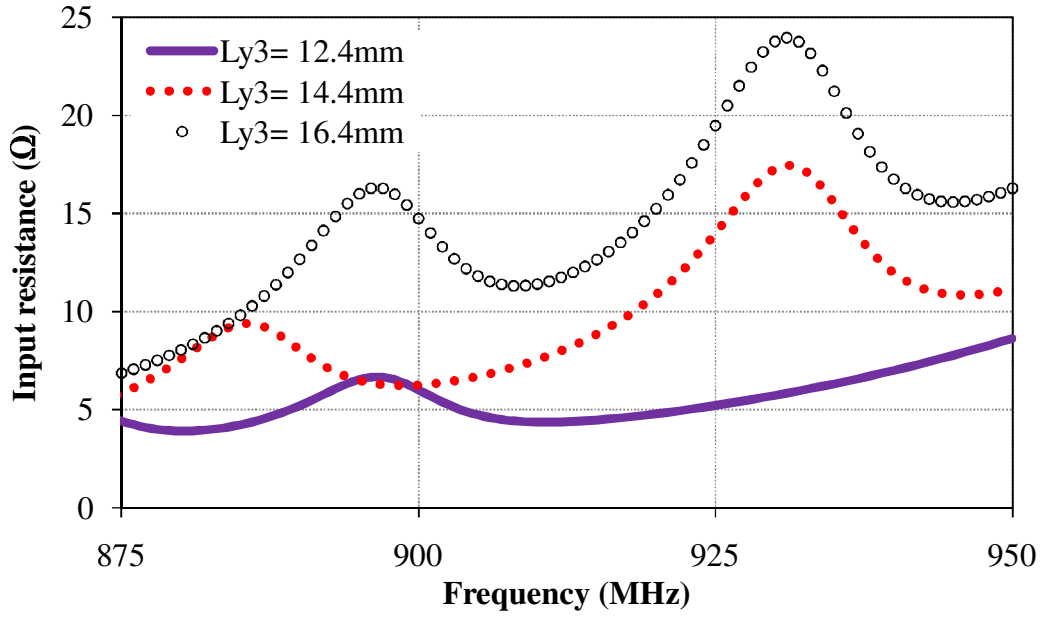

(a)

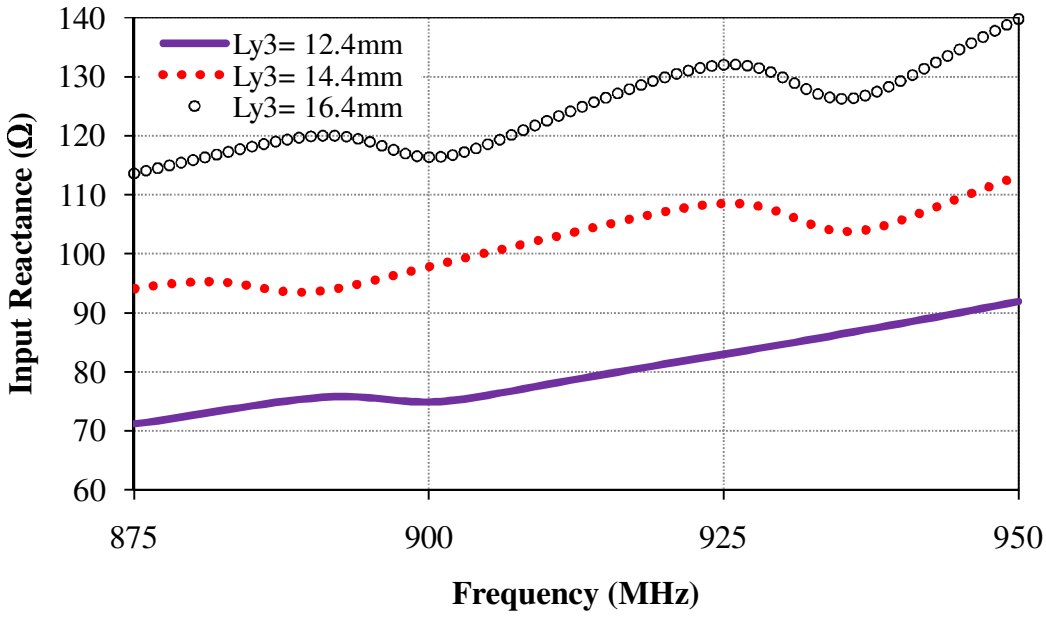

(b)

Figure 4.12: (a) Simulated Input resistance and (b) Input reactance of receiving antenna by tuning Ly3.

The effect of tuning of the width of the meandered slot on the impedance of Antenna-I is presented in Figure 4.13. It is observed that with the increase of the width of the slot both real and imaginary parts of the input impedance increase at 915 MHz and 925 MHz.

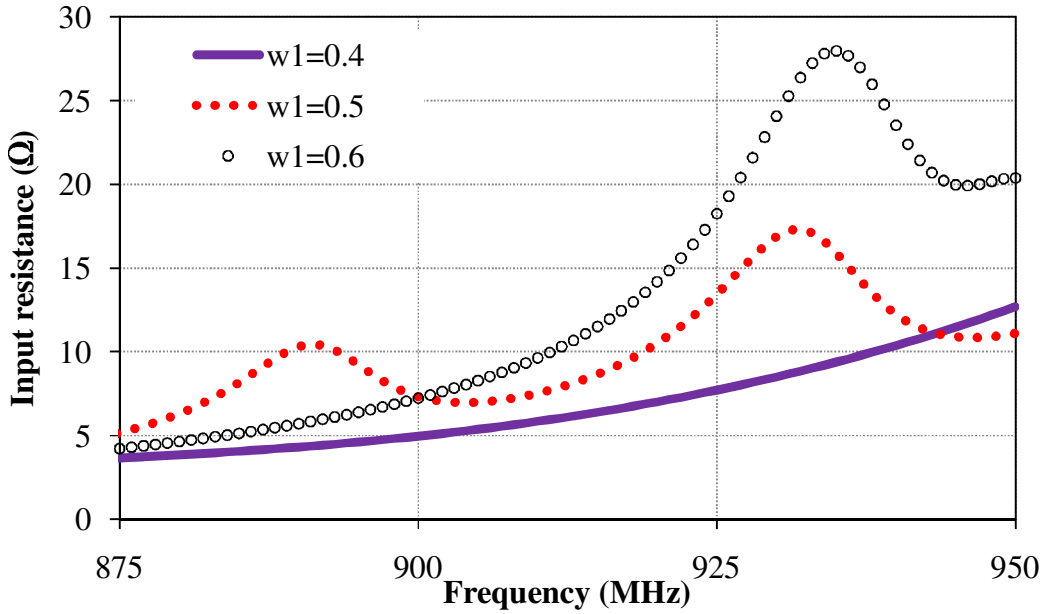

(a)

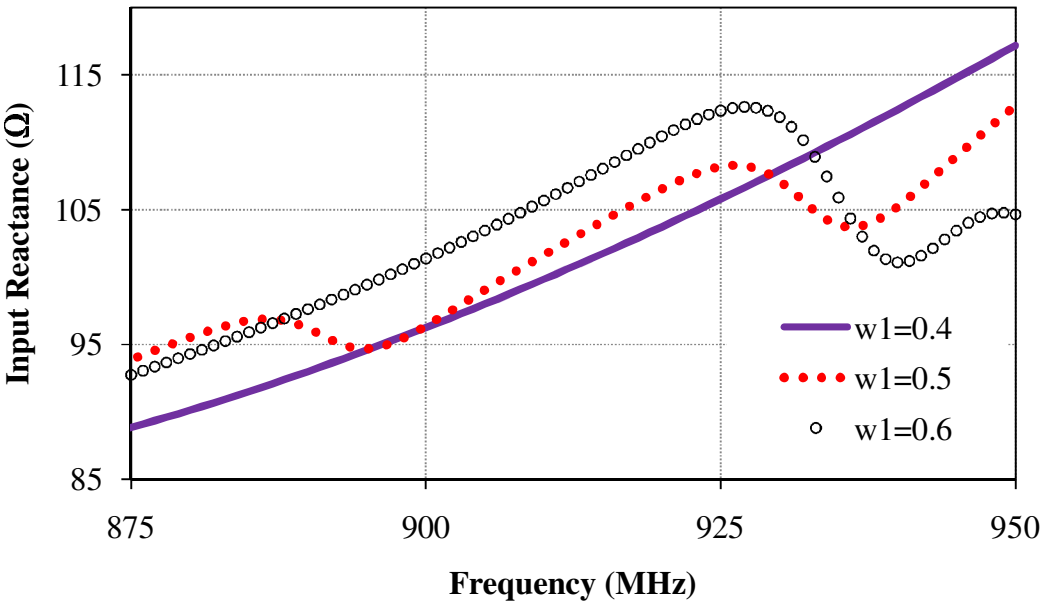

(b)

Figure 4.13: (a) Simulated Input resistance and (b) Input reactance of receiving antenna by tuning w1.

4.3.1.2. Backscattering antenna

The parametric study of the backscattering antenna is carried out in the presence of the receiving antenna under the complex conjugate matched condition at operating band. The shape parameters of the backscattering antenna are optimized in such a way that to satisfy the equation 2.6 so that in the backscattering mode, the imaginary part of the backscattering antenna should be close to zero for maximum differential RCS.

Figures 4.14 (a-c) show the variations of the imaginary part of the input impedance of the backscattering antenna with the frequency under the conjugate matched condition of receiving antenna, by tuning (at a time one parameter) Ly10, w2 and Lx4 respectively, and keeping optimized values of the other parameters. It is observed that in all the cases the zero reactance value of the backscatter antenna is -1.5 Ω for optimized shape parameters which satisfy the equation 2.6. It indicates that the backscatter antenna is properly work in the backscattering mode of the RFID tag.

4.3.2 Simulation and Measurement Results

The complete measurement setup is shown in Figure 4.15. The *S*-parameters are measured with the help of differential probe which is connected to the terminals of the antenna.

Figure 4.16 shows the simulated and measured results of the input impedance of receiving antenna (Antenna-I). The measured and simulated input impedance at 925 MHz are observed as 16+j97 Ω and 13.5+j108 Ω, respectively. These are close to the complex conjugate of the chip impedance (13-j112Ω). Figure 4.17 shows the simulated and measured results of power reflection coefficient of Antenna-I at 925 MHz. The simulated and measured bandwidth is observed from 913-960 MHz and 913-977 MHz, respectively. It shows that the presented antenna can be operated in the broadband region from 913-960 MHz. During simulation, the input impedance of Antenna-I is observed 8.69+j102.91Ω at 915 MHz. It is close to the conjugate of the chip impedance of AD220

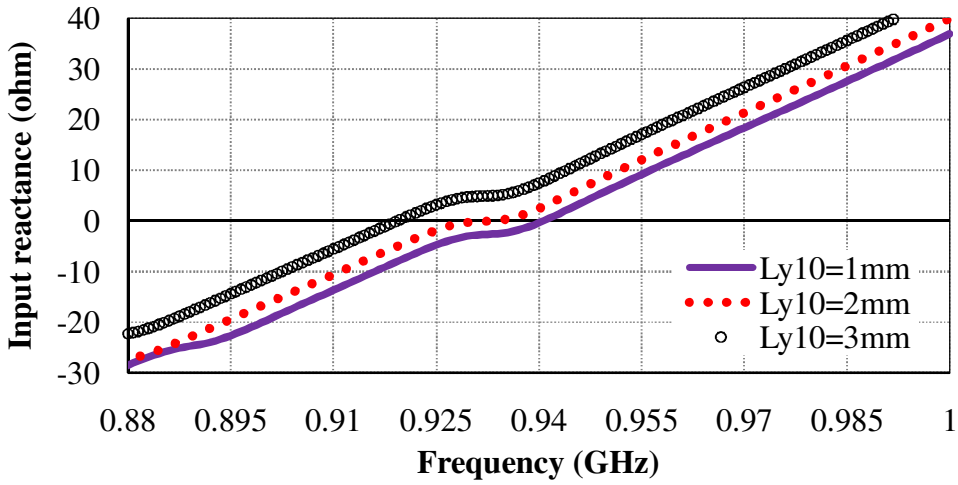

(a)

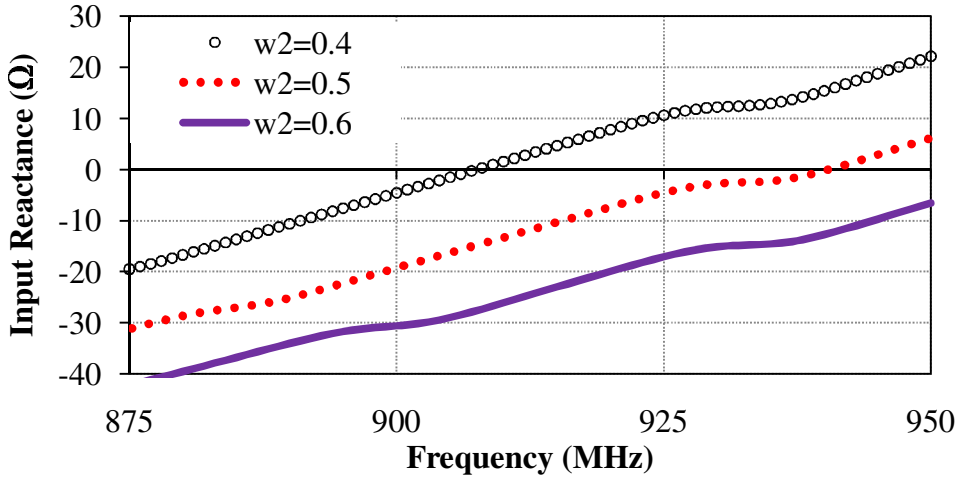

(b)

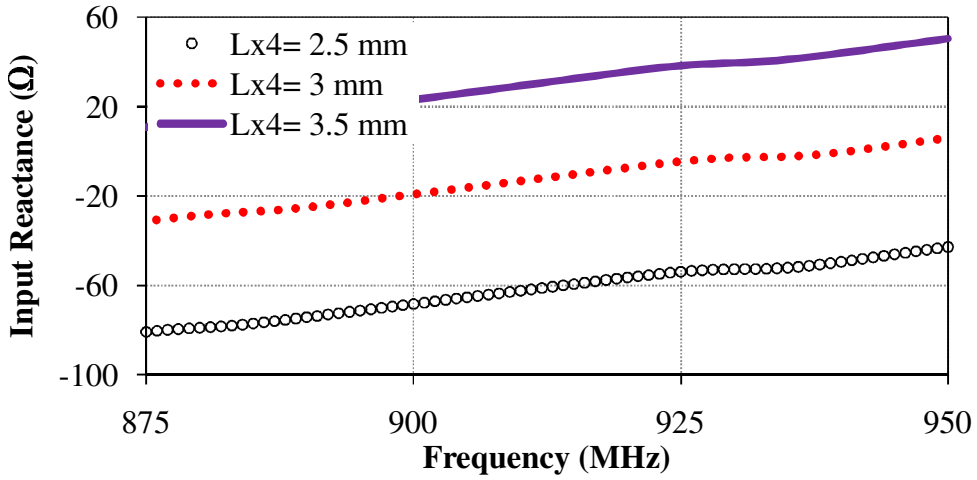

(c)

Figure 4.14: Simulated input reactance of backscattering antenna by tuning the (a) Ly10 (b) w2 and (c) Lx4

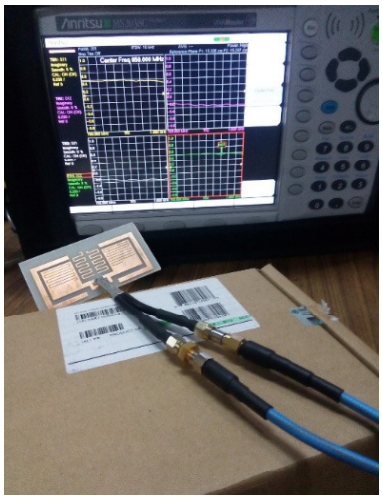

Figure 4.15: Measurement setup for S_{11} measurement

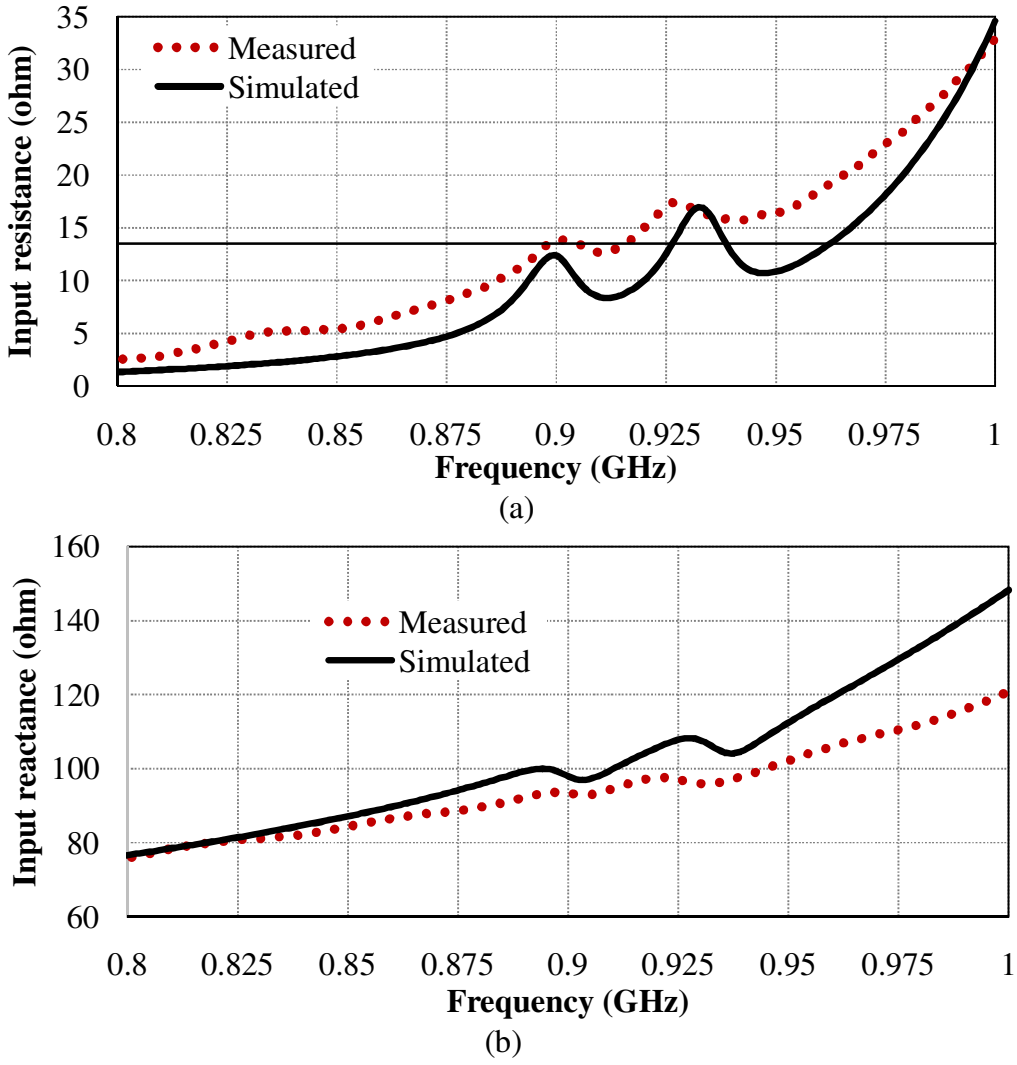

Figure 4.16: Simulated and measured input impedance variation of receiving antenna (a) resistance and (b) reactance.

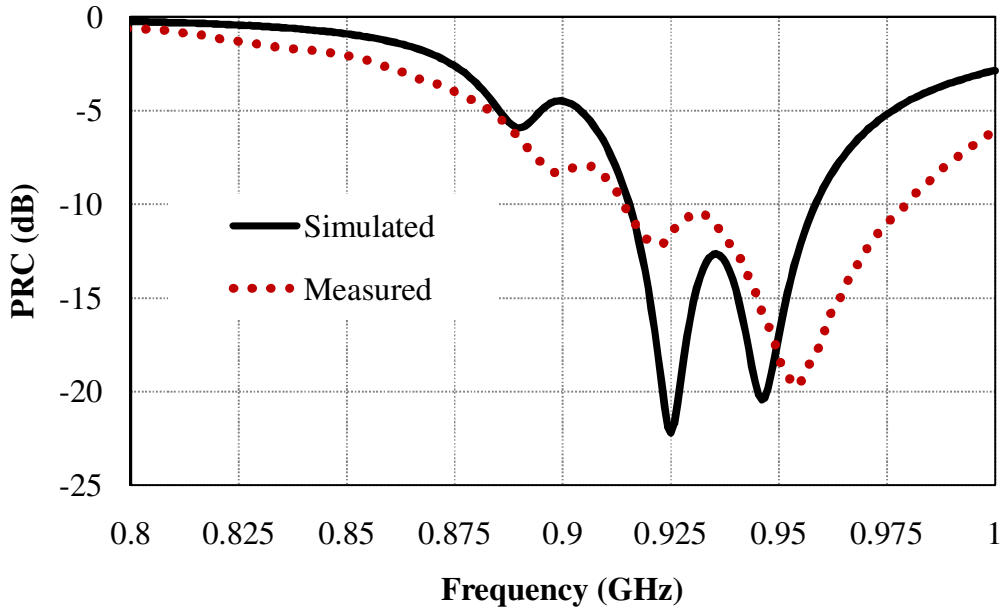

Figure 4.17: Simulated and measured power reflection coefficient variation of receiving antenna at 925 MHz

with chip impedance of 8-j91Ω. Therefore, the presented antenna can also be work with AD220 chip [Avery Dennison (2016)].

The read range of the RFID tag antenna is proportional to the differential radar cross section (RCS) (Δσ) of an antenna under two different impedance states during the backscattering operation [Chen *et al.* (2011)b]. The RCS of proposed dual Antenna at 925 MHz (impedance states: short-circuit; Z_L=0 and open-circuit; Z_L=∞) is compared with conventional single antenna structure (impedance states: short-circuit; Z_L=0 and conjugate match; Z_L=13-j110) in Figure 4.18. This value of Δσ in two states of the conventional antenna are between 38 and 25 dBsm at 925 MHz is observed as 13 dBsm. Furthermore, in the case of dual antenna structure Δσ between 38 and -73 dBsm at 925 MHz is observed as 98 dBsm. It is clear that Δσ increased from 13 to 111 dBsm at 925 MHz. The differential RCS (Δσ) in two different states (open and short) of proposed dual-antenna structure at 925 MHz is increased, which results in enhancement of read range from 4.3 to 5.9 m as shown in Figure 4.19. It is also noticed that the Antenna-I of proposed dual-antenna structure is conjugate matched and the backscattered antenna alternatively switches between open and short circuits.

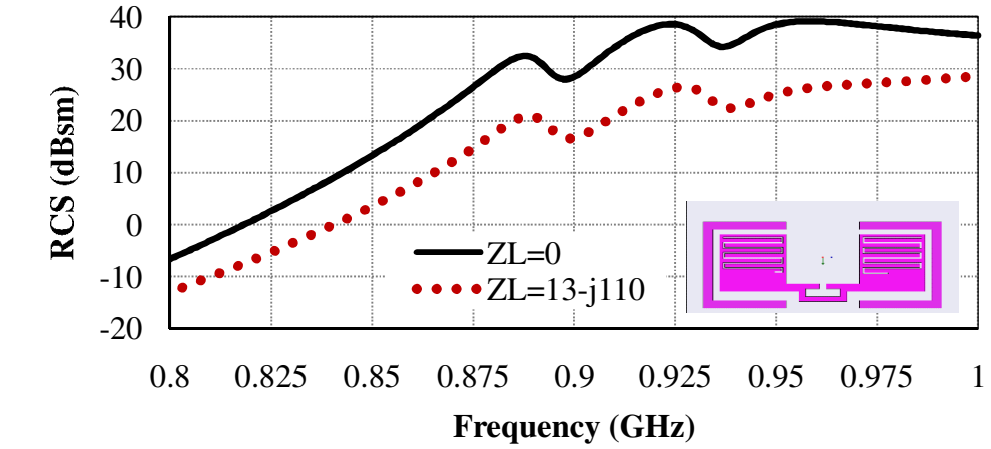

(a)

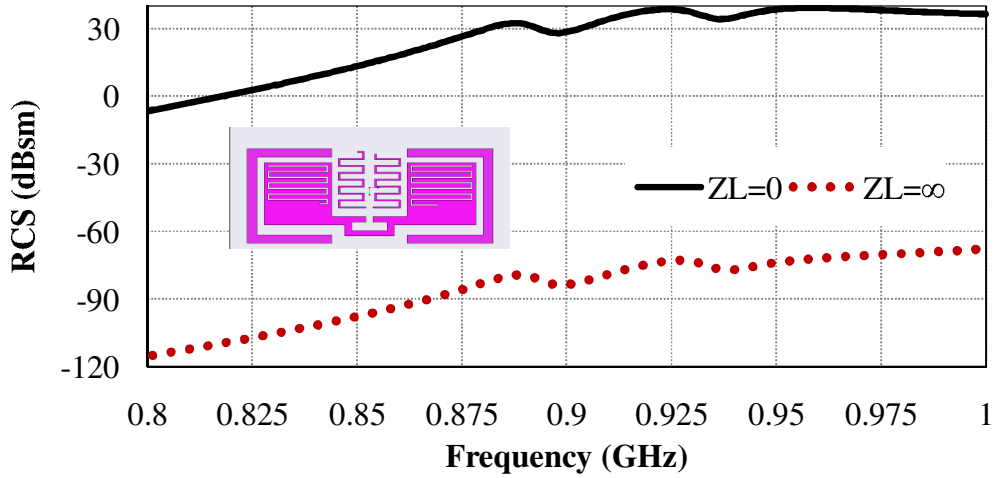

(b)

Figure 4.18: RCS variation of (a) conventional single antenna and (b) proposed antenna at 925 MHz.

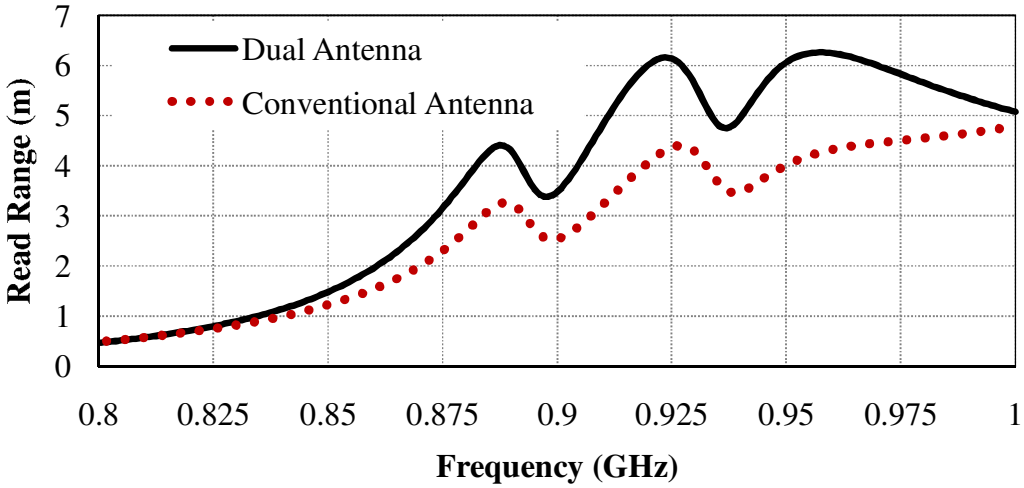

Figure 4.19: Read range comparison of conventional and proposed antenna for UHF band.

Figure 4.20 shows the radiation patterns in both *xz*-plane and *yz*-plane of receiving (Antenna-I) of RFID tag at 925 MHz. It is observed that at 925 MHz, dumbbell shaped pattern is observed in both the planes.

Figure 4.21 shows the surface current of the antenna at 925 MHz. It is observed that at 925 MHz, the whole antenna is responsible for radiation.

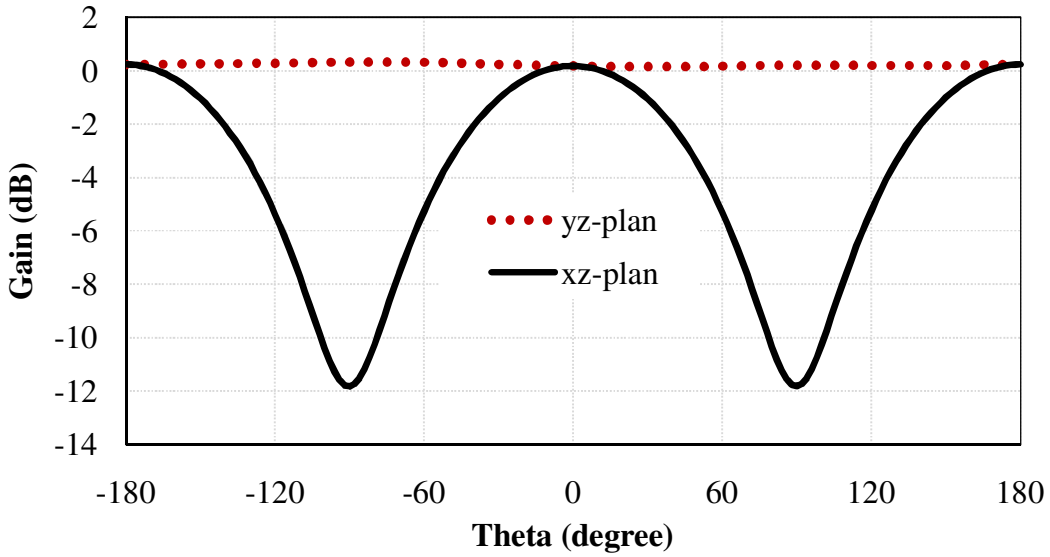

Figure 4.20: Radiation pattern of Antenna-I (receiving antenna) at 925 MHz.

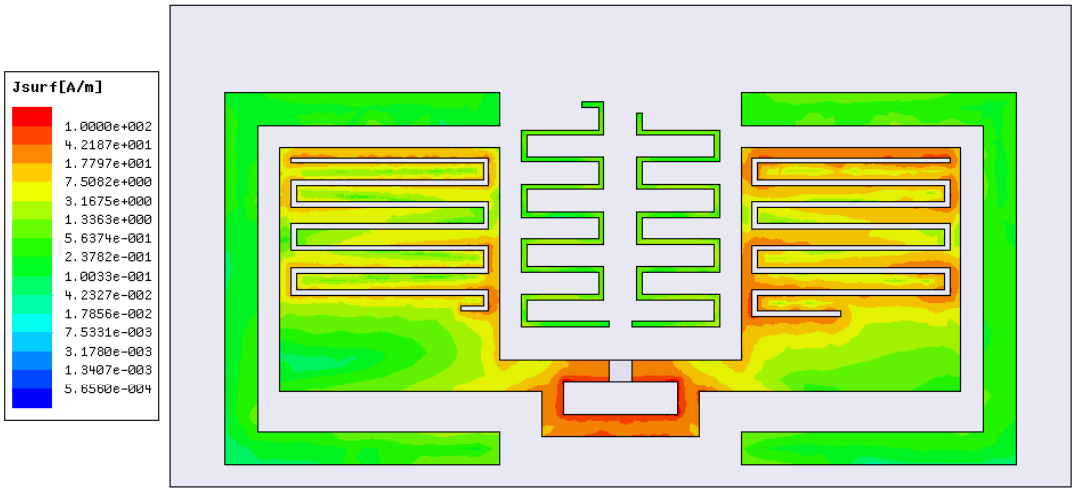

Figure 4.21: Surface current of antenna at 925 MHz

4.3.3. Effect of mounting material on RFID tag antenna

To investigate the effect of the different material on which RFID tag antenna to be mounted, the input impedance of the antenna is simulated on plastic, paper and metallic surfaces, which is shown in Figure 4.22. The electrical properties of the material are given in Table 3.3 It is observed that the input impedance will not change significantly on plastic and paper surfaces, but the significant effect is observed when the antenna is mounted on the metallic surface. Therefore, the presented antenna is suitable for mounting on paper, cardboard, and plastic materials.

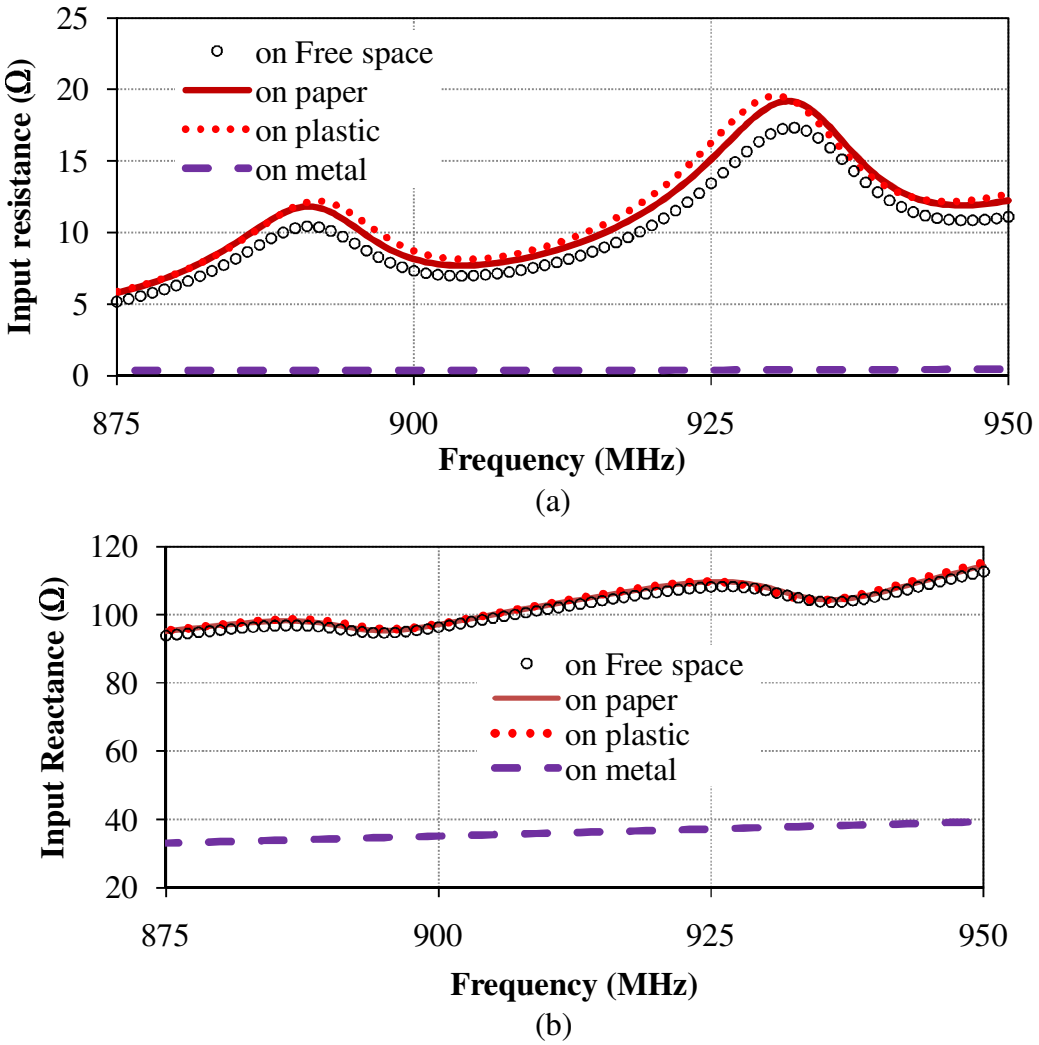

Figure 4.22: Input (a) resistance and (b) reactance of antenna on free space, paper, plastic and metal

4.4. Summary

A broadband single sided RFID tag antenna operating in the UHF band is presented. The proposed antenna utilized dual antenna structure by having simulated and measured bandwidth from 913-960 MHz and 913-977 MHz respectively which cover all of UHF band in different countries. Due to the use of dual antenna structure, the differential RCS increases, which results in enhancement of the read range at 925 MHz. Maximum read range of the proposed antenna is found to be 5.9m at 925 MHz. The measured and simulated results are in good agreement with respect to input impedance of the antenna at 925 MHz.